Molecular Mechanism of Transport Selectivity Across the Nuclear Pore Complex

Annual Report for
Blue Waters Allocation

Aleksei Aksimentiev – Principal Investigator

October 23, 2017

Center for the Physics of Living Cells
Department of Physics
University of Illinois at Urbana-Champaign

Executive summary

The nuclear pore complex (NPC) serves as a gatekeeper, regulating biomolecular transport across the nuclear envelope. The key barrier to nuclear transit is the central channel of the NPC, composed of disordered nucleoporins, or Nups. Despite experimental advances, the underlying microscopic mechanism of nuclear transport and architecture of the NPC's central channel remain largely unknown. Through a set of molecular dynamics simulations, we characterized the structural and electrical properties of the NPC diffusion barrier. The ionic conductivity of Nup proteins in solution was found to depend non-linearly on Nup concentration, approaching zero as protein content reaches 70%. A dual-resolution computational method was applied to obtain a set of realistic all-atom models of the entire biological NPC each containing approximately 140 million atoms, validated by comparing the simulated and experimentally-measured ionic conductivity of the NPC. The dual-resolution NPC model sets the stage for subsequent studies of selective molecular transport.

Confidentiality

This report includes confidential or restricted information. Please share its contents only with the Blue Waters team and National Science Foundation.

Description of research activities and results

Key challenges

The nuclear pore complex (NPC) serves as a gatekeeper, controlling the molecular traffic into and out of the nucleus of a mammalian cell. The central channel of the NPC is composed of intrinsically-disordered proteins known as Nups, which are essential elements enabling selective transport through the nuclear pore. Because of their complex and rather fragile structure, NPCs are challenging to investigate *in vivo* or reconstitute *in vitro*. Hence, experimentalists have developed synthetic analogs of NPCs that can mimic the selective transport of proteins while providing control over the environmental conditions and ability to directly detect passage of biomolecules [1, 2]. Over the past several years, advances in electron microscopy have greatly increased our knowledge of the NPC scaffolding [3, 4], but the structural architecture of the central channel has remained elusive.

Why it Matters

The evolutionary development of the nucleus has lead to the protection and compartmentalization of the genetic material between cell divisions. Passage across the nuclear envelope, known to be regulated by NPCs, is therefore of fundamental importance to eukaryotic life. A number of human diseases—including cancer, viral infections, and neurodegenerative diseases [5, 6, 7]—are caused by disturbances in the nuclear pore transport. However, the molecular details of nuclear transport have thus far remained largely unknown, in part because traditional experimental techniques cannot characterize the NPC's central channel containing disordered proteins. The simulations performed by our team on Blue Waters have produce the first atomic-resolution model of the NPC system, elucidating the architecture of the central channel. The model sets the stage for future investigation of selective molecular transport, which may offer insight into the molecular origin of several diseases and lead to the development of novel gene therapies.

Why Blue Waters

Building the microscopic model of the disordered central channel of the NPC and validating the model through calculations of the NPC ion conductivity required explicit solvent all-atom MD simulations. Because of the immense size of the all-atom NPC model—140 million atoms in total—such MD simulations are only possible on a supercomputer with the computational power of Blue Waters. The large number of compute nodes equipped with the graphics processing units connected by the fast Gemini interconnect have made Blue Waters one of the best publicly available systems for performing simulations of the entire NPC.

Accomplishments

Using a 986,600 node-hour allocation (JQ5 project), we performed three large-scale simulations that characterized the structure and ion conductivity of the NPC. First, we performed explicit-solvent all-atom MD simulations of an array of small bulk nucleoporin systems, determining ion conductivity as a function of Nup density. Second, we carried out a large set of coarse-grained Brownian dynamics simulations of the NPC central channel, representing the NPC outer scaffolding [4] and the nuclear envelope [8] using a grid-based potential. Third, based on the outcome of the coarse-grained simulations and the experimental data, we built and simulated several complete all-atom models of the biological NPC—each being 140 million atoms in total—including the outer scaffold, the disordered central channel of Nups, the nuclear envelope, and surrounding solvent. Using the ensemble of the all-atom structures, we have estimated the ion conductance of the NPC. Three presentations have

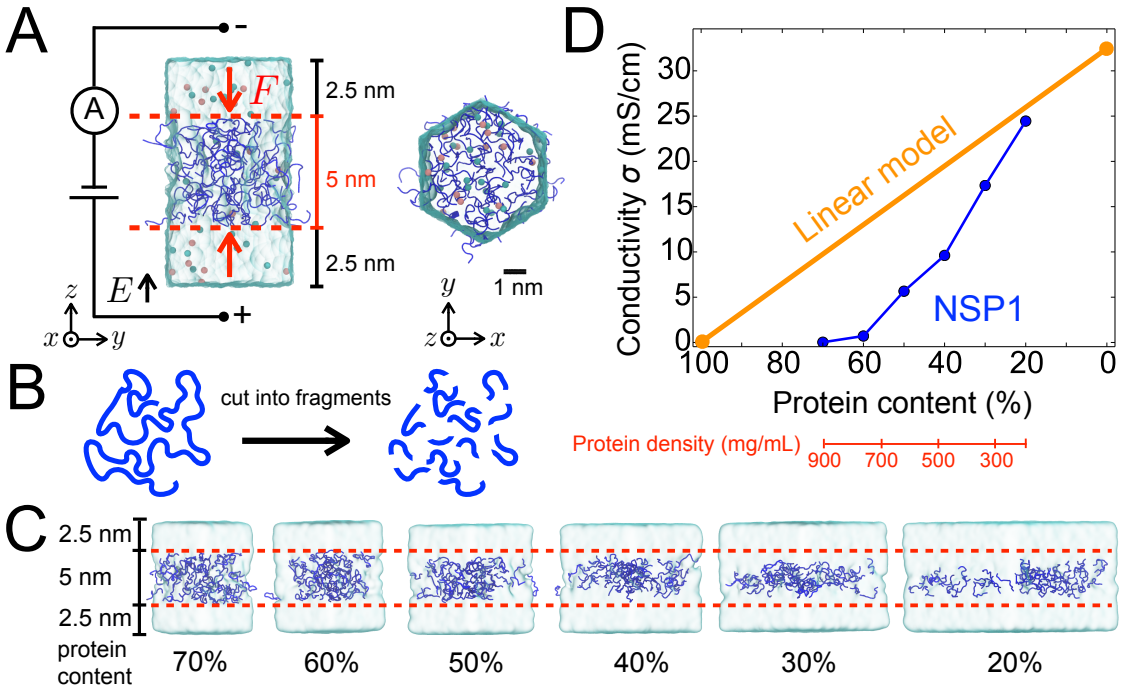

Figure 1: **MD simulations of ion conductivity of bulk nucleoporin systems.** (A) Simulation setup. The non-structured protein 1 (NPS1, dark blue tubes) is surrounded by water (semi-transparent blue surface) and ions (pink and cyan spheres). Half-harmonic potentials (red dashed lines) are applied only to the protein, keeping it within the central region of the simulation system. A 500 mV transmembrane bias is applied across the region containing NPS1. (B) To facilitate conformational sampling the NSP1 protein containing 637 amino-acids is cut into 12-residue fragments. (C) Ensemble of bulk nucleoporin systems differing by the protein content. The protein content was calculated as the ratio of the number of non-hydrogen atoms of the protein to the total number of non-hydrogen atoms within the central region of the simulation system. (D) Ion conductivity σ as a function of protein content. The linear model (orange line) indicates the expected conductivity of the central region partially occupied by the 0.15 M KCl solution. The protein density is provided below the protein content axis for reference.

been delivered to communicate our simulation results. A manuscript detailing our findings is being prepared for publication.

A1 The effect of nucleoporin density on ion conductivity.

To characterize the ion conductivity of the central pore region as a function of the Nup protein density, we performed explicit-solvent all-atom MD simulations of bulk nucleoporin systems. An individual Nup protein (non-structured protein 1; NSP1) was submerged in an electrolyte solution and confined to remain within the central volume of the system; the system was effectively infinite within the xy-plane under the periodic boundary conditions, Fig. 1A. The NSP1 constructs were cut into fragments (Fig. 1B) to expand the conformational space explored. Several simulation systems were constructed to vary the protein content within the central volume from 20 to 70%, in increments of 10% by maintaining the thickness of the protein-rich compartment constant and modifying the x and y dimensions of the simulation

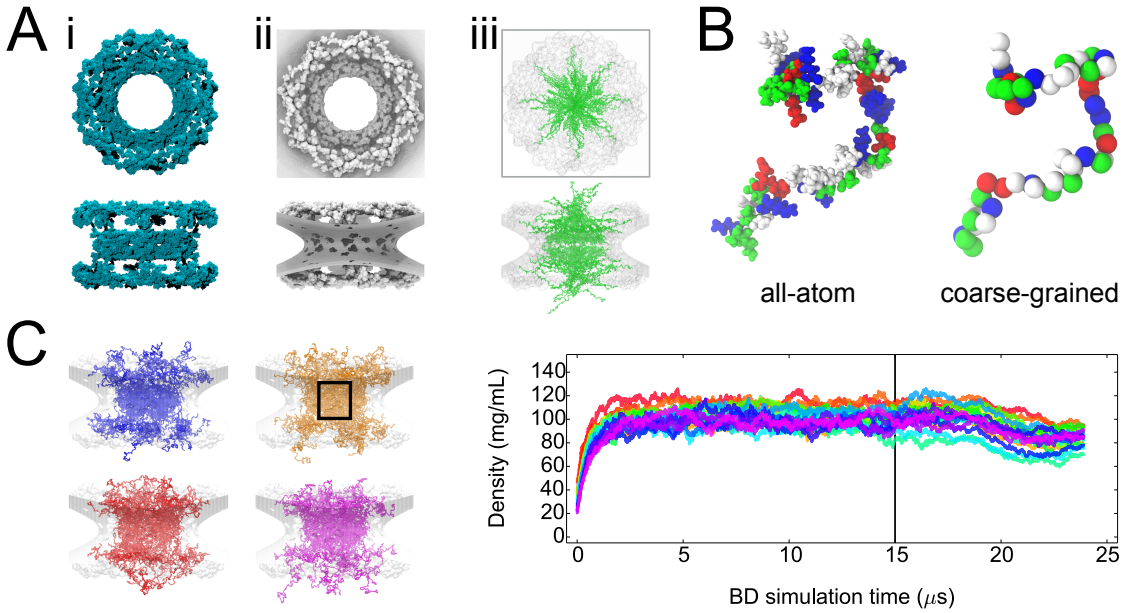

Figure 2: **Coarse-grained simulations of the nuclear pore complex.** (A) Procedure for building coarse-grained models of the NPC. All-atom coordinates derived from experiment (*i*, in cyan), combined with a hyperboloid curved surface, were used to build a potential to represent the NPC scaffold and nuclear envelope (light gray in *ii*; semi-transparent in *iii*). Random walk configurations were generated for the FG-repeat regions of nucleoporins Nup145N, Nsp1, Nup57, Nup49, and Nic96 (*iii*, in green). (B) Comparison of the coarse-grained model of a Nup protein [9, 10] (1 bead per protein residue) and the all-atom model of the same protein. Residues colored by type. (C) Brownian dynamics simulations of the NPC systems. Examples of final conformations are shown to the left. The right graph plots the density of a central pore volume (black rectangle; left) as a function of the simulation time for several Brownian dynamics trajectories. The coarse-grained potentials were softened within the first 15 μs of the simulations to enhance conformational sampling and then were gradually brought back to produce realistic representative models of the central NPC region.

system (Fig. 1C). Following minimization and equilibration, the systems were simulated under an external electric field that produced the ionic current through the system. The NSP1's ion conductivity is found to increase non-linearly with decreasing protein content (Fig. 1D). Furthermore, we observed a transition from conducting to not conducting states at a critical Nup density (at a protein content of ∼70%, Fig. 1D), matching the key experimental result obtained using the bio-mimetic NPC constructs [2].

A2 Coarse-grained simulations of the nuclear pore complex.

Through a series of Brownian dynamics simulations, we determined the architecture of the central channel of the NPC. For these simulations we used an in-house developed GPU-accelerated BD software package called Atomic Resolution Brownian Dynamics. Starting from a potential based on experimental data (Fig. 2A i,ii) and randomly-generated configurations for the central channel (*e.g.* Fig. 2A iii), Brownian dynamics simulations were performed using a one-bead per protein residue CG model developed by the Onck laboratory [9, 10], Fig. 2B. The diffusivity and potential between neighboring bonded residues were modified in several steps. In a process similar to simulated annealing, enhanced diffusion, high temperature, and weakened bonds were employed for the first 15 μs of the simulation, and then diffusion and temperature were gradually reduced, and bonds strengthened, over the final 8 μs, ending with the parameters defined by Onck's model. 20 unique conformations were generated for the central mesh network of the NPC, and equilibration was monitored by measuring the density of a central volume (Fig. 2C; black rectangle) as a function of the simulation time, Fig. 2C right. Although the protein density converged to 85 ± 15 mg/mL over the course of 23 μs, the ensemble of endpoint configurations exhibits considerable structural heterogeneity, Fig. 2C left, which we used to obtained a statistically significant estimation of the NPC's ionic conductivity.

A3 All-atom structure and ion conductance of the entire nuclear pore complex.

Ultimately, explicit solvent all-atom MD simulations were required to characterize the electrical properties of the nuclear pore complex. Therefore, we built a complete all-atom model of the biological NPC (Fig. 3A). The outer scaffolding of the NPC was generated from the all-atom model built by Lin *et al.* [4]. The conformations of the central FG-Nup mesh were derived by mapping the coarse-grained representations from the Brownian dynamics simulations to the all-atom representations. The overall shape of the lipid bilayer was determined by fitting a hyperboloid surface to a cryo-EM density map that includes the nuclear envelope (EMD-3103) [8]. Using the *lipidwrapper* tool [11], many copies of an equilibrated, solvated lipid bilayer of diphytanoyl phosphatidylcholine (DPhPC) were placed to cover the hyperboloid surface. Blocks of pure TIP3P water were then added to cover the entire system space, measuring ∼1250 × 1250 × 1500 Å^3; waters within 3 Å of protein or lipids atoms were then removed to prevent clashes. TIP3P waters were then chosen randomly and replaced with K^+ and Cl^- ions to neutralize the system and reach a 0.150 M concentration. The entire NPC system measured 140 million atoms in total, one of the largest all-atom biological systems

built to date. The assembled system was simulated in all-atom detail using NAMD2 [12], periodic boundary conditions, the CHARMM36 force field for protein [13], the TIP3P model of water [14], and custom CHARMM-compatible parameters for ions [15]. The ionic conductances of the all-atom models, Figure 3B, was estimated using a theoretical protocol described in a recent publication from our lab [16]. The average conductance of about 40 nS is within the range of experimentally-determined values (∼30 to 60 nS) [17, 18, 19], which validates our all-atom model.

List of publications and presentations associated with this work

- Winogradoff D., Maffeo C., Si W. and Aksimentiev A. Structure and ionic conductivity of the nuclear pore complex. manuscript in preparation
- (Presentation) Winogradoff, D. The Molecular Mechanism of Transport Selectivity Across the Nuclear Pore Complex. Blue Waters Symposium, Sunriver, OR May 2017
- (Presentation) Winogradoff, D. Structure and ionic conductivity of the nuclear pore complex. Conference on Biomotors, Virus Assembly, and Nanobiotechnology Applications, the Ohio State University August 2017
- (Poster) Winogradoff D., Maffeo C., Si W. and Aksimentiev A. Structure and ionic conductivity of the nuclear pore complex. Conference on Biomotors, Virus Assembly, and Nanobiotechnology Applications, the Ohio State University August 2017

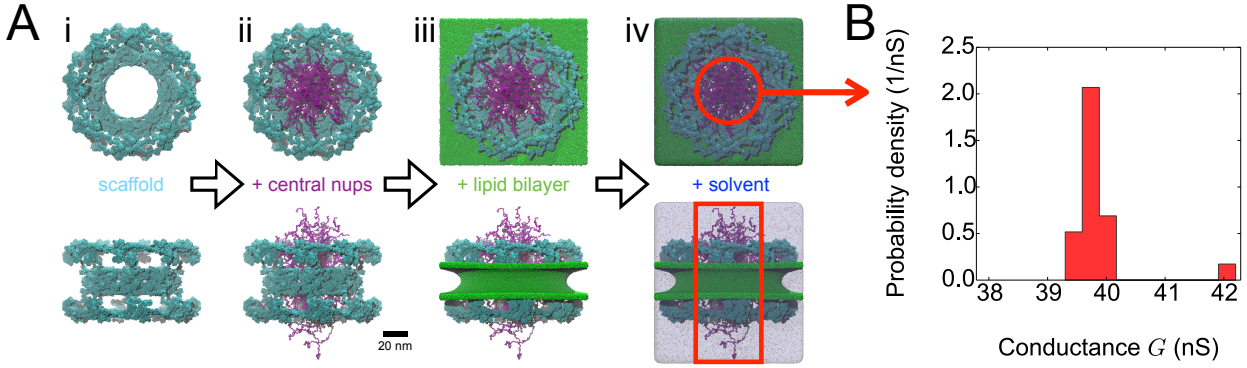

Figure 3: **All-atom model and ionic conductance of the entire nuclear pore complex.** (A) Building an all-atom model of the nuclear pore complex. Colors highlight components of the biological NPC: the outer scaffold (*i*; cyan), the central channel of Nups (*ii*; purple), curved lipid bilayer (*iii*; green), and explicit surrounding solution (*iv*; blue). (B) A histogram of the NPC ion conductance estimated from the ensemble of all-atom conformations. The volume used for the ionic current calculations is outlined in red in Panel A.

References

[1] T. Jovanovic-Talisman, J. Tetenbaum-Novatt, A. S. McKenney, A. Zilman, R. Peters, M. P. Rout, and B. T. Chait. Artificial nanopores that mimic the transport selectivity of the nuclear pore complex. *Nature*, 457:1023–1027, 2009.

[2] S. W. Kowalczyk, A. Y. Grosberg, Y. Rabin, and C. Dekker. Modeling the conductance and DNA blockade of solid-state nanopores. *Nanotechnology*, 22:315101, 2011.

[3] K. H. Bui, A. von Appen, A. L. DiGuilio, A. Ori, L. Sparks, M.-T. Mackmull, T. Bock, W. Hagen, A. Andrés-Pons, J. S. Glavy, et al. Integrated structural analysis of the human nuclear pore complex scaffold. *Cell*, 155:1233–1243, 2013.

[4] D. H. Lin, T. Stuwe, S. Schilbach, E. J. Rundlet, T. Perriches, G. Mobbs, Y. Fan, K. Thierbach, F. M. Huber, L. N. Collins, A. M. Davenport, Y. E. Jeon, and A. Hoelz. Architecture of the symmetric core of the nuclear pore. *Science*, 352:aaf1015, 2016.

[5] V. Le Sage and A. J. Mouland. Viral subversion of the nuclear pore complex. *Viruses*, 5:2019–2042, 2013.

[6] A. Köhler and E. Hurt. Gene regulation by nucleoporins and links to cancer. *Molecular cell*, 38:6–15, 2010.

[7] A. Jovičić, J. Mertens, S. Boeynaems, E. Bogaert, N. Chai, S. B. Yamada, J. W. Paul III, S. Sun, J. R. Herdy, G. Bieri, N. J. Kramer, F. H. Gage, L. Van Den Bosch, W. Wim Robberecht, and A. D. Gitler. Modifiers of c9orf72 dipeptide repeat toxicity connect nucleocytoplasmic transport defects to ftd/als. *Nature neuroscience*, 18:1226–1229, 2015.

[8] A. von Appen, J. Kosinski, L. Sparks, A. Ori, A. L. DiGuilio, B. Vollmer, M.-T. Mackmull, N. Banterle, L. Parca, P. Kastritis, K. Buczak, S. Mosalaganti, W. Hagen, A. Andres-Pons, E. A. Lemke, P. Bork, W. Antonin, J. S. Glavy, K. H. Bui, and M. Beck. In situ structural analysis of the human nuclear pore complex. *Nature*, 526:140, 2015.

[9] A. Ghavami, L. M. Veenhoff, E. van der Giessen, and P. R. Onck. Probing the disordered domain of the nuclear pore complex through coarse-grained molecular dynamics simulations. *Biophysical journal*, 107:1393–1402, 2014.

[10] A. Ghavami, E. van der Giessen, and P. R. Onck. Coarse-grained potentials for local interactions in unfolded proteins. *Journal of chemical theory and computation*, 9:432–440, 2012.

[11] J. D. Durrant and R. E. Amaro. Lipidwrapper: an algorithm for generating large-scale membrane models of arbitrary geometry. *PLoS computational biology*, 10:e1003720, 2014.

[12] J. C. Phillips, R. Braun, W. Wang, J. Gumbart, E. Tajkhorshid, E. Villa, C. Chipot, R. D. Skeel, L. Kale, and K. Schulten. Scalable molecular dynamics with NAMD. *Journal of Computational Chemistry*, 26:1781–1802, 2005.

[13] K. Hart, N. Foloppe, C. M. Baker, E. J. Denning, L. Nilsson, and A. D. MacKerell, Jr. Optimization of the CHARMM additive force field for DNA: Improved treatment of the BI/BII conformational equilibrium. *Journal of Chemical Theory and Computation*, 8:348–362, 2012.

[14] W. L. Jorgensen, J. Chandrasekhar, J. D. Madura, R. W. Impey, and M. L. Klein. Comparison of simple potential functions for simulating liquid water. *The Journal of Chemical Physics*, 79:926–935, 1983.

[15] J. Yoo and A. Aksimentiev. Improved parametrization of Li^+, Na^+, K^+, and Mg^{2+} ions for all-atom molecular dynamics simulations of nucleic acid systems. *Journal of Physical Chemistry Letters*, 3:45–50, 2012.

[16] W. Si and A. Aksimentiev. Nanopore sensing of protein folding. *ACS Nano*, 11:7091–7100, 2017.

[17] J. Bustamante, J. Hanover, and A. Liepins. The ion channel behavior of the nuclear pore complex. *Journal of Membrane Biology*, 146:239–251, 1995.

[18] T. Danker, H. Schillers, J. Storck, V. Shahin, B. Krämer, M. Wilhelmi, and H. Oberleithner. Nuclear hourglass technique: an approach that detects electrically open nuclear pores in xenopus laevis oocyte. *Proceedings of the National Academy of Sciences*, 96:13530–13535, 1999.

[19] M. Mazzanti, J. O. Bustamante, and H. Oberleithner. Electrical dimension of the nuclear envelope. *Physiological Reviews*, 81:1–19, 2001.